J Neurophysiol 99: 2985–2997, 2008.
First published April 9, 2008; doi:10.1152/jn.01098.2007.

Dopamine Increases the Gain of the Input-Output Response of Rat Prefrontal Pyramidal Neurons

Kay Thurley, Walter Senn, and Hans-Rudolf Lüscher
Department of Physiology, University of Bern, Switzerland

Submitted 3 October 2007; accepted in final form 1 April 2008

Thurley K, Senn W, Lüscher H-R. Dopamine increases the gain of the input-output response of rat prefrontal pyramidal neurons. *J Neurophysiol* 99: 2985–2997, 2008. First published April 9, 2008; doi:10.1152/jn.01098.2007. Dopaminergic modulation of prefrontal cortical activity is known to affect cognitive functions like working memory. Little consensus on the role of dopamine modulation has been achieved, however, in part because quantities directly relating to the neuronal substrate of working memory are difficult to measure. Here we show that dopamine increases the gain of the frequency-current relationship of layer 5 pyramidal neurons in vitro in response to noisy input currents. The gain increase could be attributed to a reduction of the slow afterhyperpolarization by dopamine. Dopamine also increases neuronal excitability by shifting the input-output functions to lower inputs. The modulation of these response properties is mainly mediated by D1 receptors. Integrate-and-fire neurons were fitted to the experimentally recorded input-output functions and recurrently connected in a model network. The gain increase induced by dopamine application facilitated and stabilized persistent activity in this network. The results support the hypothesis that catecholamines increase the neuronal gain and suggest that dopamine improves working memory via gain modulation.

INTRODUCTION

Prefrontal cortical function subserves higher-order cognitive processes, including working memory, i.e., the mental ability to transiently store and manipulate information which guides forthcoming actions. The cellular correlate of working memory is thought to consist of sustained reverberating activity in prefrontal neurons after stimulus removal (Goldman-Rakic 1995). Dopamine (DA) is an important neuromodulator that supports working memory. In fact, antagonists of the DA D1 receptor dramatically reduce the performance of monkeys in various working-memory tasks (Sawaguchi and Goldman-Rakic 1991). DA is released by dense projections from the ventral tegmental area to the prefrontal cortex (PFC) (Seamans and Yang 2004).

Incited by the importance of the prefrontal cortex and DA for working memory, a huge number of studies, dealing with DA actions in prefrontal cortical areas, has emerged during the last decades (for review, see Seamans and Yang 2004). In general, DA has been found to enhance the excitability of prefrontal pyramidal neurons mediated by D1 receptor stimulation (e.g., Henze et al. 2000; Lavin and Grace 2001; Shi et al. 1997; Tseng and O'Donnell 2004; Yang and Seamans 1996; but see Gulledge and Jaffe 1998). This was assumed to stabilize working memory activity and gave rise to numerous modeling studies (for review, see e.g., Cohen et al. 2002; Durstewitz et al. 2000b; Wang 2001).

The present study gives insight into DA modulation of the intrinsic response properties of individual PFC pyramidal neurons, which are relevant for understanding persistent activity. Neuronal response properties can best be characterized by means of the input-output response function, i.e., the *f-I* curve, giving the rate of action potential discharge as a function of the injected current strength. An important computational feature of the neuronal transfer function is the modulation of its gain (i.e., the maximal slope of the *f-I* curve), which may either stabilize or switch working memory (Salinas and Sejnowski 2001). Gain modulation of neocortical layer 5 pyramidal neurons has been shown to arise from distal dendritic input (Larkum et al. 2004) and noisy input (Arsiero et al. 2007; Higgs et al. 2006) and has been described as a result of serotonin or noradrenaline application (Higgs et al. 2006; Zhang and Arsenault 2005). Gain increase by DA was reported by Lavin and Grace (2001) for short stimuli that evoke only a few spikes. Here we extend their findings by showing an even larger increase of neuronal gain for long-lasting quasi-stationary responses that are relevant for self-sustained network activity. Moreover, the synaptic input a neuron experiences in vivo is characterized by random fluctuations rather than a DC current. Because noisy inputs have been shown to reduce the gain of the neuronal response function (Chance et al. 2002; Rauch et al. 2003; Shu et al. 2003), this might counteract DA-mediated gain increase found with square pulses. We provide evidence that, nevertheless, DA increases the gain of the input-output function of prefrontal pyramidal neurons for noisy inputs. In addition, DA shifts the *f-I* curve to the left, i.e., to lower input currents. Together with previous results on neuronal gain modulation by serotonin or noradrenaline (Zhang and Arsenault 2005), our data support the idea put forward by Servan-Schreiber et al. (1990) that catecholamines modulate the gain of PFC neurons and, at the network level, increase the signal-to-noise ratio of the information transmission. Incorporating our findings into a recurrently connected model network shows that the DA modulation stabilizes the sustained activity underlying working-memory functions. A DA-induced gain increase therefore synergistically supports the previously described stabilization of persistent activity by dopaminergic modulation of synaptic transmission (Compte et al. 2000; Durstewitz et al. 2000a).

Address for reprint requests and other correspondence: K. Thurley, Dept. of Physiology, University of Bern, Buehlplatz 5, CH-3012 Bern, Switzerland (E-mail: thurley@pyl.unibe.ch).

The costs of publication of this article were defrayed in part by the payment of page charges. The article must therefore be hereby marked "*advertisement*" in accordance with 18 U.S.C. Section 1734 solely to indicate this fact.

METHODS

Experimental preparation and electrophysiological recordings

All experimental procedures were performed according to the *Ethical Principles and Guidelines for Experiments on Animals* of the Swiss Academy of Medical Sciences. Coronal slices (300 μm) containing the medial PFC (see, e.g., Yang et al. 1996) were prepared from 17- to 44-day-old Wistar rats (with 80% of the data from rats >30 days). The preparation procedure is described in detail in Rauch et al. (2003). Whole cell patch-clamp recordings were taken from the soma of layer 5 PFC pyramidal neurons. Series resistance and capacitance were compensated using the bridge balance and capacitance neutralization of the amplifier (BVC-700A, Dagan, Minneapolis, MN). Layer 5 medial PFC pyramidal neurons with their thick apical dendrite were identified under visual guidance using infrared differential video microscopy. Selection was electrophysiologically confirmed by means of the regular-spiking behavior and passive membrane properties, after whole cell patch-clamp mode was established (Zhang 2004). Patch pipettes were filled with (in mM) 130 K-gluconate, 5 KCl, 10 HEPES, 4 ATP-Mg, 0.3 Na_2-GTP, and 10 Na_2-phosphocreatine, pH adjusted to 7.3 with KOH. Pipette solution additionally contained 0.2% biocytin to reconstruct cell morphology after recording. Experiments were conducted at 34–35°C.

Stimulation protocol

Stimulation currents were designed according to an Ornstein-Uhlenbeck stochastic process to mimic in vivo synaptic barrage (for a detailed description, see Rauch et al. 2003). Such a process yields a good approximation for the spike distribution observed in higher cortical areas during stimulus evoked activity (e.g., Aggelopoulos et al. 2005) or during working memory (e.g., Compte et al. 2003). There is also some direct indication that the synaptic barrage in vivo matches an Ornstein-Uhlenbeck process (Destexhe and Paré 1999). The statistics of such currents are characterized by a Gaussian distribution with mean m, a SD s and by a correlation time τ. We fixed the correlation time $\tau = 3$ ms to resemble fast excitatory and inhibitory synaptic inputs. Current-clamp protocols of the present kind have been shown to result in negligible distortions of neuronal response functions compared with conductance-clamp experiments (LaCamera et al. 2004; Rauch et al. 2003). Thus a recorded neuron responds in a similar way to either current injection or conductance drive and using technically less demanding current-clamp methods, turns out to be reasonable.

The principal experimental protocol was as follows: stimulus trains with constant mean current m and SD s were injected, and the neuronal response frequency f was calculated as the total spike number divided by the stimulus duration. Recordings were not included in the analysis in case of considerable changes of spike amplitude and shape in the response (Rauch et al. 2003). Different trains were separated by several tens of seconds, depending on the concrete protocol (see following text), to let the cell recover after stimulation. First, the mean input current m was increased stepwise from a subthreshold value until the emission of a single or a few spikes. That gave the current threshold for spiking, i.e., the rheobase current (Rauch et al. 2003). Then in the current interval between threshold and *f-I* curve saturation (Arsiero et al. 2007), stimuli with different means m were chosen and injected in random order to prevent temporal correlations. About 30% of the values of m were repeated once or twice.

Two different protocols were used for the recordings. First, we recorded data for a SD $s = 100$ pA. The value 100 pA was arbitrarily chosen. It is, however, in a range comparable with other studies (Arsiero et al. 2007; Rauch et al. 2003). Single stimulus trains lasted 10 s. The break between pulses was 50–60 s. Recording one *f-I* curve took roughly 30 min.

In a second series of experiments, we recorded data for three different values of the SD s using a modified version of the previous protocol. At first, the response curve for $s = 50$ pA was determined. Then two other values of s were chosen as the values that gave responses of 5 and 10 Hz at rheobase current for $s = 50$ pA, respectively. Stimulus trains were shortened to 6 s. Shorter stimulation times necessitated shorter times for recovering, i.e., 30–40 s instead of 50–60 s. With that protocol, recording *f-I* curves for three different SDs s took ~30 min as well.

In addition, membrane resting potential and access resistance were monitored by injection of a hyperpolarizing square pulse (100 ms, −50 to −150 pA) preceding each noisy stimulus train. Recordings have been discontinued in case of large drifts, i.e., membrane potential changes more than ±3 mV, despite unmodified experimental conditions, or the series resistance exceeding 20 MΩ. The membrane time constant was determined by an exponential fit to the recovering voltage response after the square pulse.

Pharmacology

To exclude transient responses, recordings started 5–10 min after drug application (regarding the dependence of DA influence on application time, see also RESULTS). Application continued during data acquisition to ensure stable drug levels, mimicking the in vivo situation of tonic rather than phasic DA presence. Recording the *f-I* curve under drug treatment took ~30 min. By the end of the data acquisition under drug treatment, each cell was already held for almost 1.5 h. A washout of ≤30 min followed the period of drug application in case the recording remained stable (evaluated by means of membrane potential and series resistance). No consistent washout results were obtained for any of the substances (data not shown). Concentrations were as follows (in μM): 25, 50, or 100 DA always including 0.2% sodium bisulfite to prevent oxidation, 5 SKF 38393, 10 SCH 23390, 10 quinpirole, and 10 or 50 sulpiride.

In most experiments, synaptic currents were systematically blocked. Bicuculline (10 μM) was applied to block $GABA_A$ receptor-mediated currents. To suppress glutamatergic inputs, 6-cyano-7-nitroquinoxalene-2,3-dione (CNQX, 10 μM; to block AMPA receptors) and 2-amino-5-phosphonovaleric acid (APV, 50 μM, to block NMDA receptors) were used in all experiments with DA concentrations at 25 or 50 μM. For DA application (100 μM), experiments without synaptic blockers gave similar results and were therefore pooled with experiments under synaptic blockade—no significant differences were found in the changes of *f-I* curve parameters with ($n = 5$) and without ($n = 8$) synaptic blockers, i.e., in the transient and steady state phase $P \gg 0.05$ for rheobase shift, gain change, and change of maximum firing rate, one-way ANOVA, see also *Data analysis and statistics*). In experiments with DA anta-/agonists, glutamatergic currents were blocked with the unspecific glutamate receptor antagonist kynurenate (1 mM). DA modulation of the slow afterhyperpolarization (sAHP) was investigated without synaptic blockers in all cases.

Data analysis and statistics

The analysis of the experimentally measured input-output functions makes use of the constant leakage integrate-and-fire neuron with a floor (CLIFF) (see Fusi and Mattia 1999). The CLIFF neuron was shown to describe the firing pattern of pyramidal neurons in rat somatosensory cortex (Rauch et al. 2003). It also accounts well for our PFC data, obtained with a single SD s of the input current (but see Arsiero et al. 2007). The temporal development of the membrane voltage V is described by

$$C\frac{dV}{dt} = -\lambda + I(t) \qquad (1)$$

with the effective membrane capacitance C, the leakage λ and the input current $I(t)$. The spike threshold of the model neuron was set to $\theta = -45$ mV. Additionally, the model requires a reset value V_r after

spiking and a refractory period τ_r. To complete the neuron model, one needs to define a lower bound, the floor, which we set to −65 mV. For an input current according to an Ornstein-Uhlenbeck process, the firing rate f of the CLIFF neuron is given by (Fusi and Mattia 1999)

$$f(m) = \left[\tau_r + \frac{\theta - V_r}{m - \lambda} C + \frac{\tau s^2}{(m-\lambda)^2} \left(e^{-\frac{m-\lambda}{\tau s^2} C\theta} - e^{-\frac{m-\lambda}{\tau s^2} C V_r} \right) \right]^{-1} \quad (2)$$

Numerical values for the set of free parameters $\{\lambda, V_r, C, \tau_r\}$, i.e., CLIFF *f-I* curves, were determined by fitting *Eq. 2* to the experimental *f-I* curves. By means of the fitted CLIFF *f-I* curves, we numerically determined: the rheobase current, which was defined as the largest mean input current m with firing rate $f(m) = 0$, the gain of the *f-I* curve, i.e., of the $f(m)$ function, which was given by the maximum of the first derivative (slope) of $f(m)$, and the maximum firing rate, which we defined to be in physiological range at $f(m_{max})$ with m_{max} = 700 pA + rheobase current according to the first parameter. Differences in the three parameters were evaluated between the *f-I* curves before and during drug application. Then, the significance level was determined using Student's *t*-test, one- or two-way ANOVA. To evaluate statistical correlations, Pearson's linear correlation coefficient r was used.

Experiments on the sAHP: stimulation protocol and analysis

For the experiments on the sAHP, we followed the protocol used by Higgs et al. (2006). The resting potential of a cell was held at −65 mV, and exactly 30 spikes were triggered with 2-ms square pulses at 50 Hz. The amplitude of the sAHP was estimated by averaging the voltage trace of the membrane potential between 450 and 550 ms after the last action potential (see also Fig. 4*A*).

Steady-state analysis of recurrently connected neurons

The analysis of the network of recurrently connected integrate-and-fire neurons follows the approach of Brunel (2000). It offers a simplified mean field theory, based on the *f-I* curve of the single cells of a network, and provides a tool to study the impact of the modulation of the single-cell *f-I* curve on network behavior. We investigate a recurrently connected network of N CLIFF neurons with parameters given by the average of the n = 13 recorded cells in the DA (100 μM) application experiments. Neurons are connected with a probability c. A single neuron receives input from as well as provides output to the network it is embedded in. The basic assumption in mean field theory is that in a homogeneous group of neurons in a network, a single cell reflects the average behavior of all cells in that homogeneous group. Therefore one can look at the response dynamics of a single cell exemplarily for the whole group. Like in the simulations (see following text), our network consists of one group of neurons, only. The activity state of each neuron is characterized by its firing rate $f = f(m)$ as a function of the mean input m (*Eq. 2*) and satisfies the self-consistent equation

$$m = cN\tau_c J(f - f_{sp}) + m_{sp} \quad (3)$$

where c is the average fraction of presynaptic neurons targeting a postsynaptic neuron, N the total number of neurons, τ_c the current decay time constant, J the average connection strength, and f_{sp} the spontaneous firing rate in response to the spontaneous background current m_{sp}. As a simplification, the SD of all currents is expected to be constant and unaffected by the state of the network and any input. The mean input m_{sp} contains a contribution from the recurrent excitatory network, which fires with frequency f_{sp}, and an additional external current that reflects summed excitatory and inhibitory input. Note that we keep the level of spontaneous activity f_{sp} the same for dopaminergic and nondopaminergic cases, i.e., we adjust the corresponding spontaneous background current m_{sp}. Otherwise, an excitability increase would obviously enhance the response to background input, which would counteract if not abolish bistability and thus storing working-memory items. Therefore we use the assumption of stable spontaneous activity independent of the responsiveness in our model, without explicitly modeling its emergence. Such adjustment of spontaneous activity levels can be interpreted as balancing activity from inhibitory interneurons. It is known that D1 agonists also enhance the amplitude and the frequency of GABAergic inputs to PFC pyramidal neurons (Seamans and Yang 2004; Seamans et al. 2001b). Other modeling studies showed that this might not only keep spontaneous activity constant but rather may lead to the reduction of the latter (Durstewitz and Seamans 2002; Durstewitz et al. 2000a)—an assumption recently confirmed experimentally (Lavin et al. 2005). Thus assuming the level of spontaneous activity to be independent of DA influence is justified. A decrease of spontaneous activity levels would even pronounce our results because it widens the basins of attraction for persistent activity, which further enhances stability (Durstewitz and Seamans 2002).

A stable state in the network is reached when the output frequency f of each neuron together with external inputs provides enough current to the network to evoke the same output again. In terms of our exemplary single cell, this condition is fulfilled at the intersection of the *f-I* curve (*Eq. 2*) with a line obtained by rewriting *Eq. 3* to the form

$$f = (m - m_{sp})/(cNt_c J) + f_{sp} \quad (4)$$

The intersections are fixed points of the system. Looking for the points of intersection provides the possibility to investigate the appearance and modulation of bistability, i.e., the coexistence of states of spontaneous and persistent activity, in dependence on parameters that characterize the network.

Simulations of recurrently connected integrate-and-fire neurons

We constructed a network of n = 260 CLIFF neurons with parameters given by the n = 13 recorded cells in the DA application experiments. The sets of parameters were in equal numbers assigned to the model neurons. For each neuron i, the input current $I(t)$ in *Eq. 1* consists of contributions from inside (recurrent) and outside the network. The recurrent contribution is chosen as $I(t) = \Sigma_j J_{ij} \Sigma_k \exp((t - t_j^{(k)} - d)/\tau_c)\Theta(t - t_j^{(k)} - d)$, with $\Theta(t)$ denoting the Heaviside step function, $\Theta(t) = 1$ for $t \geq 0$, and $\Theta(t) = 0$ otherwise. The value of $t_j^{(k)}$ gives the time when the presynaptic neuron j emitted the kth spike, which is received by neuron i after a delay d = 1 ms. For each connection from a neuron j to a neuron i, the connection strength J_{ij} was chosen to be $J_{ij} = J > 0$ with probability c = 0.1, and $J_{ij} = 0$ otherwise. Hence we have a purely excitatory network. Note that J_{ij} is measured in pA. The current time constant τ_c = 25 ms was set to overcome the long refractory period obtained by the fit and reflects the importance of NMDA receptors in stabilizing persistent activity (Wang 1999). External inputs reflecting items to be stored in working memory or distracting inputs are provided by DC injections. Additionally background activity, composed of contributions from inside and outside the network, results in an input current of a mean m_{sp} in each neuron that evokes a spontaneous firing rate f_{sp}. We keep the level of spontaneous activity f_{sp} the same for dopaminergic and nondopaminergic cases, i.e., we adjust the corresponding spontaneous background current m_{sp}. The SD of the background current was set to 100 pA.

RESULTS

DA-mediated increase of excitability

Prefrontal cortical layer 5 pyramidal neurons (Fig. 1*A*) were injected with noisy currents, which resemble synaptic barrage in vivo (see METHODS). We determined the input-output rela-

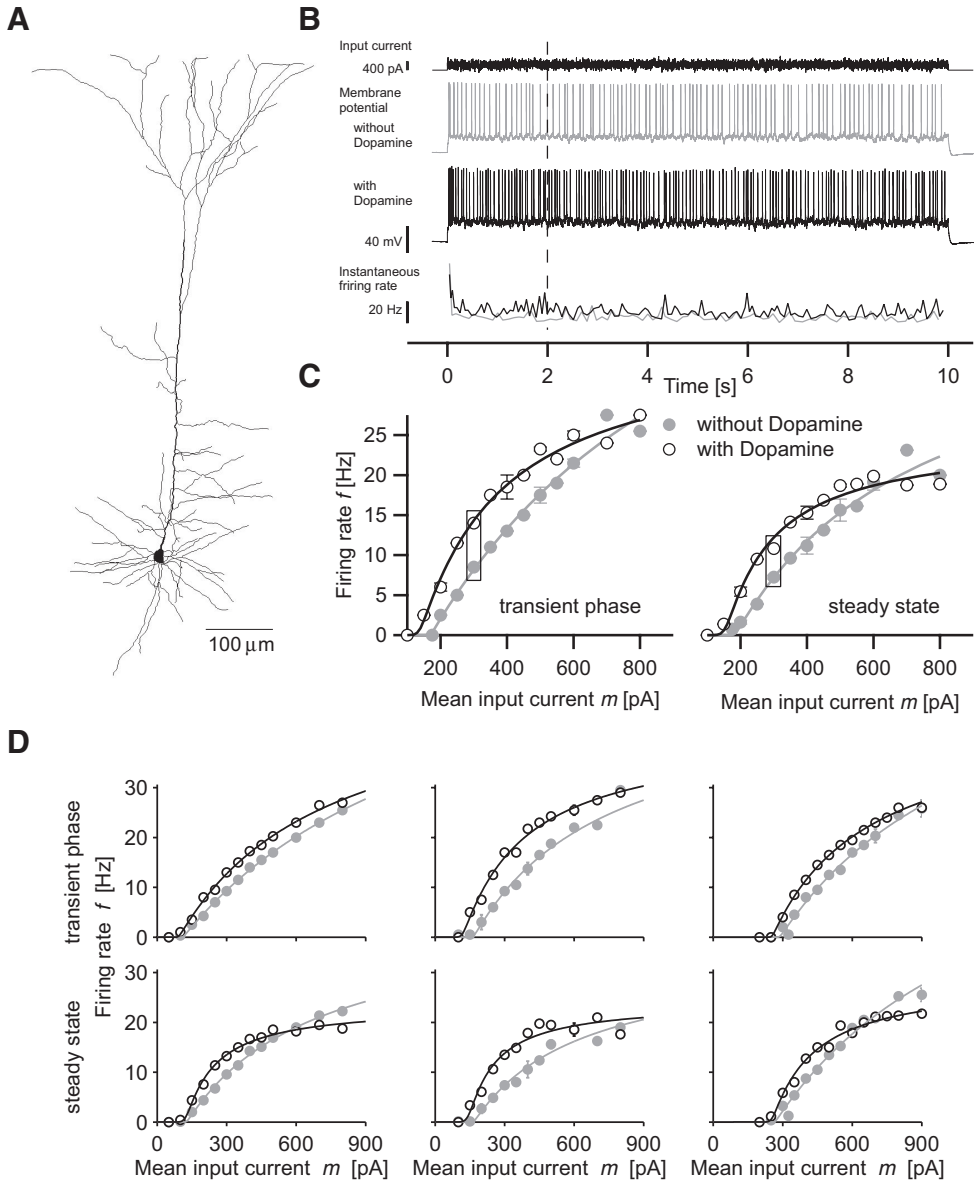

FIG. 1. Dopamine differentially affects layer 5 pyramidal neurons in the prefrontal cortex (PFC). *A*: reconstruction of a layer 5 PFC pyramidal neuron. *B*: example of the noisy current stimulus with a mean of 250 pA (*top*) and corresponding voltage traces before (*2nd panel*) and during (*3rd panel*) dopamine application. *Bottom*: the instantaneous firing rate. - - -, division of response phases that were defined as transient and steady-state response. *C*: example of the influence of dopamine on the response curve of a layer 5 PFC pyramidal neuron. Curves are given for the transient phase at the beginning of the stimulation (*left*) and for the steady-state response (*right*). ●, data before dopamine application; ○, values during application. The SD (error bars) is given in case the stimulus was repeated at the particular value of m (30% of the values). —, fits of the data with the CLIFF model neuron. □, values belonging to the traces in the *top panels*. *D*: 3 further examples of modulation of PFC pyramidal cell response by dopamine (DA). A DA concentration of 100 μM was used in the experiments shown in the figure.

tionship (*f-I* curve) of the cells before and during DA application, measuring the frequency of action potential discharge in response to different mean input currents (Fig. 1*B* gives an example). The first 1–2 s of the response of neocortical pyramidal neurons to long-lasting stimulation have been shown to comprehend temporally variable components due to processes on short time scales like spike frequency adaption and facilitation (LaCamera et al. 2006; Rauch et al. 2003). After the first few seconds the response stays quasi-stationary until the end of stimulation, i.e., the response frequency changes negligible subsequently, apart from possible slow spike frequency adaption. However, pyramidal cells are not able to sustain high output rates for very large depolarizing inputs, limiting the range of suitable values for the mean input current m (Rauch et al. 2003). The appropriate range of mean input currents depends on properties of the particular cell such as its input resistance and was adapted for each experiment (see also METHODS).

For the analysis, we divided the neural response into two parts: a transient phase consisting of the first 2 s of the response and the subsequent part, which we refer to as "steady" state (Fig. 1*B*). We discuss the principle findings by means of the example shown in Fig. 1*C*: the results were similar between transient phase and steady state—except for absolute firing frequencies, which were higher in the transient phase because of incomplete spike frequency adaptation. At low current values, i.e., lower than ~600 pA in Fig. 1*C*, DA increased excitability through a shift of the *f-I* curve to lower current values and a gain increase, i.e., increase of the maximum slope of the *f-I* curve. For high mean input, i.e., greater than ~600 pA in Fig. 1*C*, the output frequency was decreased in the steady state, indicating lower responsiveness but not in the transient phase. Similar results were obtained in other neurons (Fig. 1*D*).

To ensure that the preceding results are not due to fluctuations in the dopaminergic modulation of neural responses, noisy current pulses of 1-s duration were injected at a rate of 0.1 Hz, and the output spikes were monitored. The mean current m was adjusted to evoke an average of roughly seven

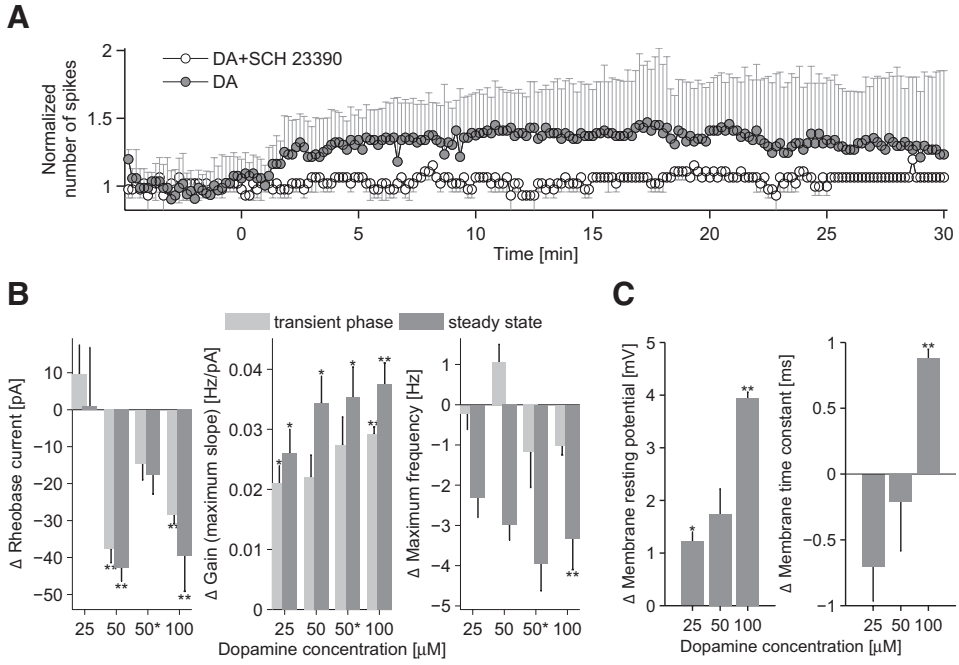

FIG. 2. Characterization of the modulation of PFC pyramidal cell response by DA. *A*: time development of pyramidal cell response to a stimulus that was fixed to trigger spikes at 7 Hz before drug application. Normalized average number of spikes ± SD of $n = 7$ cells for DA and $n = 3$ cells for DA+SCH 23390. Time point 0 is the start of application. *B* and *C*: dose-dependent changes of the parameters for the *f-I* curve, i.e., rheobase current, gain, maximum firing frequency (*B*), and for the passive membrane properties, i.e., membrane resting potential, membrane time constant (*C*). Mean values ± SE for differences between parameter pairs before and during DA application are given for the transient phase (▤) and the steady state (▨). At position 50* in *B*, values are reported for experiments with fixed resting membrane potential. *, significant differences before and during DA application: *, $P \leq 0.05$; **, $P \leq 0.01$, paired *t*-test.

spikes in response to the 1-s current pulses during the 5-min control phase prior to DA application. The SD *s* of the input current was fixed to 100 pA. Then for ~30 min, the response was recorded under DA presence (50 μM). About 2 min after the start of DA application the response increased and stabilized at higher level after ~5 min of application (Fig. 2*A*). The response remained stable for almost 25 min, although at the end of the recording it started to decrease slightly. Blocking DA D1 receptors with SCH 23390 (10 μM), occluded an excitability increase with DA (50 μM), Fig. 2*A*.

Quantification of dopaminergic f-I curve modulation

To quantify the results, we fitted the *f-I* curves with an integrate-and-fire model neuron (CLIFF) and extracted three parameters, i.e., rheobase current, as a measure of the shift of the *f-I* curve, gain (maximum slope), and maximum frequency (see METHODS). Figure 2*B* reports the DA mediated changes of *f-I* curve parameters and Table 1*A* lists the corresponding mean values and SD; see also supplemental material.[1] Experiments were conducted at three different DA concentrations, i.e., 25, 50, and 100 μM. Data for 100 μM was acquired with the "first" stimulation protocol and for 25 and 50 μM with the "second" (see *Stimulation protocol* in METHODS and *Dopamine effects remain for different amount of input fluctuations* in the following text). Therefore we analyzed *f-I* curves, which correspond to values of the SD *s* between 100 and 225 pA, in case of 25 and 50 μM DA, and to $s = 100$ pA for 100 μM DA.

The general outcome is similar for all DA concentrations, although nonsignificant (one-way ANOVA) variations between different DA concentrations are apparent. Under DA, the mean rheobase current was decreased for DA at 100 μM ($n = 13$) and 50 μM ($n = 7$) but not for 25 μM ($n = 6$). We found indications for a dose-dependent increase of the gain of the *f-I* relationship; the gain increase was larger with higher DA concentration. Both smaller rheobase current and larger gain indicate an increase of excitability evoked by DA in PFC pyramidal neurons at small input currents. Furthermore, Fig. 2*B* corroborates similar DA mediated changes of the *f-I* curves for the transient phase and the steady state. Note, however, that the gain change under DA is larger in the steady state than in the transient phase. After DA administration, the absolute values of the gain are even significantly different between transient and steady-state response (see supplemental material). The maximum firing rate decreased with increasing DA concentration during the steady-state phase; although significant only for 100 μM DA.

DA modulates passive membrane properties

To monitor the stability of the recoding, we injected hyperpolarizing square pulses, preceding each noisy current stimulus (see METHODS). That way we additionally estimated effects of drug application onto passive membrane properties (Fig. 2*C*). The membrane resting potential was increasingly depolarized for higher DA levels. The input resistance, as reflected by the membrane time constant, was increased for 100 μM and showed a tendency to decrease at lower concentrations.

Gain increase is independent of membrane potential increase

In a next set of experiments, we aimed to test if the effect of DA on *f-I* curves was independent of the accompanying membrane depolarization. Therefore we kept the cellular resting potential at −65 mV by compensating DC-current injection and recorded *f-I* curves with and without 50 μM DA (50* in Fig. 2*B* and Table 1*A*). The gain increase was in a range comparable to the experiments without fixed resting potential. The rheobase current was still reduced somewhat and the maximum firing frequency was strongly reduced although not significantly (see also DISCUSSION).

[1] The online version of this article contains supplemental data.

TABLE 1. *Characterization of the f-I curve (A) and passive membrane properties (B) without and with application of DA or its agonists and antagonists*

	Rheobase Current [pA]		Gain (maximum slope) [Hz/pA]		Maximum Frequency [Hz]		
	Before	During	Before	During	Before	During	*n*
			A. Characterization of the f-I curve				
DA							
25 μM							
t	224 ± 104	234 ± 91	0.078 ± 0.022	0.099 ± 0.035*	26.1 ± 2.4	25.9 ± 3.4	6
s	217 ± 103	218 ± 115	0.077 ± 0.024	0.103 ± 0.032*	23.2 ± 2.8	20.9 ± 4.5	
50 μM							
t	137 ± 105	99 ± 102**	0.107 ± 0.037	0.129 ± 0.021	30.5 ± 4.3	31.6 ± 6.1	7
s	140 ± 94	97 ± 97**	0.101 ± 0.01	0.136 ± 0.024*	29.4 ± 5.9	26.5 ± 4.8	
50 μM*							
t	175 ± 120	160 ± 133	0.130 ± 0.035	0.157 ± 0.047	52.1 ± 6.4	51.0 ± 8.7	4
s	165 ± 118	147 ± 137	0.124 ± 0.029	0.159 ± 0.038*	49.0 ± 6.5	45.0 ± 7.7	
100 μM							
t	151 ± 45	123 ± 45**	0.074 ± 0.016	0.104 ± 0.018**	31.0 ± 4.1	29.9 ± 4.1	13
s	155 ± 40	115 ± 48**	0.085 ± 0.022	0.122 ± 0.019**	28.6 ± 4.5	25.2 ± 4.6**	
SKF 38393	179 ± 65	147 ± 56*	0.092 ± 0.033	0.115 ± 0.025**	26.3 ± 4.7	21.6 ± 4.6**	9
Quinpirole	153 ± 56	110 ± 39**	0.086 ± 0.027	0.099 ± 0.024	24.5 ± 5.5	24.5 ± 6.8	7
DA+SCH 23390	9 ± 105	166 ± 101	0.11 ± 0.038	0.087 ± 0.023	27.9 ± 10.2	24.6 ± 8.9	4
SCH 23390	191 ± 105	186 ± 94	0.11 ± 0.038	0.112 ± 0.04	27.9 ± 10.2	23.0 ± 8.1	4
DA+Sulpiride	119 ± 64	84 ± 43*	0.102 ± 0.024	0.116 ± 0.017*	29.0 ± 8.5	25.8 ± 7.2**	6
Sulpiride	193 ± 66	207 ± 95	0.085 ± 0.030	0.085 ± 0.034	21.1 ± 2.6	21.1 ± 3.0	3

	Membrane Resting Potential [mV]		Membrane Time Constant [ms]		
	Before	During	Before	During	*n*
		B. Passive membrane properties			
DA					
25 μM	−65.4 ± 2.3	−64.2 ± 2.9*	16.2 ± 3.1	15.5 ± 2.1	6
50 μM	−67.7 ± 2.3	−66.0 ± 3.9	17.4 ± 6.5	17.2 ± 5.9	7
100 μM	−69.1 ± 3.3	−65.2 ± 3.0**	13.6 ± 3.3	14.5 ± 3.4**	13
SKF 38393	−69.3 ± 0.5	−68.9 ± 0.5	17.5 ± 0.9	18.7 ± 0.6*	8
Quinpirole	−68.0 ± 0.6	−67.2 ± 0.5	15.6 ± 0.7	16.6 ± 0.6**	7
DA+SCH 23390	−66.4 ± 4.2	−67.0 ± 4.8	12.5 ± 4.2	12.7 ± 6.1	4
SCH 23390	−66.4 ± 4.2	−66.4 ± 4.5	12.5 ± 4.2	14.4 ± 7.6	4
DA+Sulpiride	−65.7 ± 0.5	−62.9 ± 0.6**	22.4 ± 1.2	22.2 ± 1.2	6
Sulpiride	−66.0 ± 0.5	−66.9 ± 0.4	20.0 ± 1.1	19.0 ± 0.7	3

Values are means ± SD. For dopamine (DA) values for transient (t) as well as steady state (s) phases are given. Data for experiments with fixed resting membrane potential is given under the entry 50 μM*. For the DA anta-/agonists only values for the steady state are listed. In case of SCH 23390 first control data was acquired, then data in presence of SCH and finally data for DA and SCH together. A visual aid is given to quickly detect significant differences between control conditions and drug application, i.e., * for $P \leq 0.05$ and ** for $P \leq 0.01$, paired *t*-test. See supplemental material for plots of the listed values and for the parameters of the CLIFF model neuron after fitting to the experimental data.

No temporal effects underlie the excitability increase by DA

To exclude that the reported DA effects are an artifact of the experimental procedure, we recorded four cells using the same temporal protocol as in the preceding text but did not apply any drug. We found no significant change in any of the parameters, i.e., the rheobase current (from 158 ± 84 to 175 ± 72 pA, $P = 0.163$, paired *t*-test), the gain of the *f-I* curve (from 0.094 ± 0.051 to 0.086 ± 0.044 Hz/pA, $P = 0.166$, paired *t*-test), and the maximum firing rate (form 26.5 ± 8.3 to 24.8 ± 7.7 Hz, $P = 0.104$, paired *t*-test). Moreover, the minor changes, i.e., increase of the rheobase, gain decrease, and reduction of the maximum firing rate are in line with a time-dependent rundown of cellular responsiveness rather than with increased excitability as found after DA application. The time-dependent decrease of the maximum firing rate might—at least in part—account for the reduction of the maximum firing rate we found with DA application. Slow inactivation of voltage-gated sodium channels appears for strong stimuli and limits the maximum firing frequency (Fleidervish et al. 1996). Possibly sodium channel inactivation was augmented time dependently in our experiments.

D1 receptors account for most reported DA effects

To test whether DA D1 or D2 receptors are involved in the DA-mediated modulation of the *f-I* curve, we separately applied the D1 receptor agonist SKF 38393 and the D2 receptor agonist quinpirole (Table 1 and supplemental material). SKF 38393 (5 μM) modulated the *f-I* curve similar to DA and increased the membrane time constant. The membrane potential, however, was not affected. The D2 receptor agonist quinpirole (10 μM) evoked a reduction of the rheobase current and increased the membrane time constant; the other *f-I* curve parameters remained unaffected.

In a second series of experiments, we did recordings in presence of D1 (SCH 23390) or D2 (sulpiride) receptor antagonists. We applied DA (50 μM) together with SCH 23390 (10 μM). SCH 23390 blocked the effects of DA onto the *f-I* curve and passive membrane properties (Table 1 and supplemental

material). SCH 23390 applied alone did not show significant influences. Applying DA (100 μM) together with sulpiride resulted in effects on the *f-I* curve comparable with the application of DA or the D1 receptor agonist (Table 1 and supplemental material). We tested with a sulpiride level of 10 μM ($n = 4$) and 50 μM ($n = 2$) to have a DA-sulpiride ratio comparable with values from the literature (e.g., Seamans and Yang 2004). Both sulpiride levels gave similar results and were pooled for analysis. Furthermore the membrane resting potential was significantly increased, but not the membrane time constant as this was the case for the application of the D1 receptor agonist. Sulpiride (50 μM) itself showed no significant influences on the parameters of interest.

A cross-activation of nondopaminergic receptors, e.g., β-adrenergic receptors, becomes possible with the high concentrations of DA used in our experiments, i.e., 25–100 μM. Testing this possibility by blocking β-adrenergic receptors with propanolol (10 μM) reduced the effects of DA (50 μM) on the *f-I* curve and passive membrane properties (see supplemental Fig. S8 in the supplemental material). The rheobase current was still significantly reduced by DA application in presence of propanolol as well as the maximum firing rate. Under propanolol, the gain of the *f-I* curve was reduced similar to experiments without drug application, indicating temporal rundown of cellular responsiveness (see preceding text). Subsequent addition of DA increased the gain back to control levels in the steady-state phase—gain changes were, however, not significant in none of the cases: $P > 0.05$, two-way ANOVA. Note, that the experiments had been done as a single recording session, i.e., first the control *f-I* curve was measured, then the *f-I* curve with propanolol, and finally the *f-I* curve with propanolol and DA together. Passive membrane properties, i.e., membrane potential and membrane time constant, were unaffected.

Dopamine effects remain for different amount of input fluctuations

In the previous experiments, we investigated the response of layer 5 PFC pyramidal neurons to noisy input currents with only one amplitude of the input fluctuation, i.e., SD *s*. We therefore injected currents of three different amplitudes of input fluctuation into $n = 7$ cells with 50 μM DA and $n = 6$ cells with 25 μM DA, yielding qualitatively similar results as the example in Fig. 3. The features of DA modulation remain for different values of the amplitude of input fluctuations (Fig. 3, DA at 50 μM); i.e., increase of the rheobase current, gain increase, and reduced maximum firing rate is present in the transient as well as the steady-state phase.

The *f-I* curves in PFC pyramidal neurons are sensitive to the amount of input fluctuations over the whole range of input currents (Arsiero et al. 2007) and show a gain increase with increasing noise (Higgs et al. 2006). Figure 3 confirms that both features are preserved under DA presence.

Because the gain increase has been indicated to correlate with a decrease of slow spike frequency adaptation and sAHP (Higgs et al. 2006; see also following text), it might be that combination of DA with noise does not lead to an *additional* gain increase. We therefore had a closer look at the gain increase by DA at different amount of input fluctuation. The gain increase by noise was somewhat smaller after application of DA than before. It was, however, not significant (-0.0340 ± 0.0210 before and -0.0213 ± 0.0229 during DA, $P = 0.299$, one-way ANOVA).

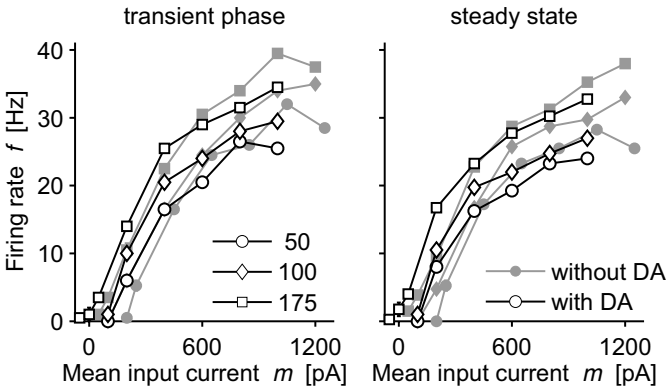

FIG. 3. Dopamine effects remain for different SD of the injected current. Three different values of the SD *s* were injected, i.e., 50 pA (circles), 100 pA (diamonds), and 175 pA (squares). Left: the response of the cell during the transient phase at the beginning of stimulation; right: the corresponding steady-state responses. Data before DA application are drawn in gray and during DA application in black.

Dopamine decreases the sAHP

The response of neocortical pyramidal neurons comprehends adaption—and facilitation—processes on several time scales from a few milliseconds up to the order of seconds (e.g., LaCamera et al. 2006; Rauch et al. 2003). The attenuating effects of noise onto slow adaptation (Tang et al. 1997) and slow afterhyperpolarization have been shown to be related to gain increase in neurons of the somatosensory cortex (Higgs et al. 2006). To test if the modulation of slow adaption might underlie the gain increase mediated by DA, we chose two different approaches.

First, we investigated DA modulation of the sAHP, using the same protocol as Higgs et al. (2006) (see also METHODS). The evoked sAHPs were reduced by application of 50 μM DA ($n = 6$, Fig. 4*A*). Estimating the amplitude of the sAHP between 450 and 550 ms after the last pulse confirmed a DA-induced reduction of the sAHP (Fig. 4*C*). The reduction was partially reversible during wash out. It decayed back to control values over time in five of seven neurons (data not shown), and after 30 min of wash out, the mean sAHP was larger than under DA treatment but still smaller than in control conditions (Fig. 4*C*). We refer to the most hyperpolarized part of the AHP as the medium AHP (mAHP, i.e., tens of to a few hundreds of milliseconds after the last action potential). DA also reduced the mAHP (see Fig. 4*A*, data not quantified). Blocking D1 receptors with 10 μM SCH 23390 only partially blocked the reduction of the sAHP by 50 μM DA (see supplemental Fig. S9). The dopaminergic reduction of the AHP has been suggested to be due to cross-activation of β-adrenergic receptors in hippocampal pyramidal neurons (Malenka and Nicoll 1986; but see Pedarzani and Storm 1995. To investigate whether such cross-activation might underlie our findings in prefrontal pyramidal cells, we blocked β-adrenergic receptors using propanolol (10 μM). The presence of propanolol occluded the reduction of the mAHP by DA (Fig. 4*B*, data not quantified). However, the sAHP was still substantially reduced by DA (50 μM) despite propanolol presence (Fig. 4, *B* and *D*).

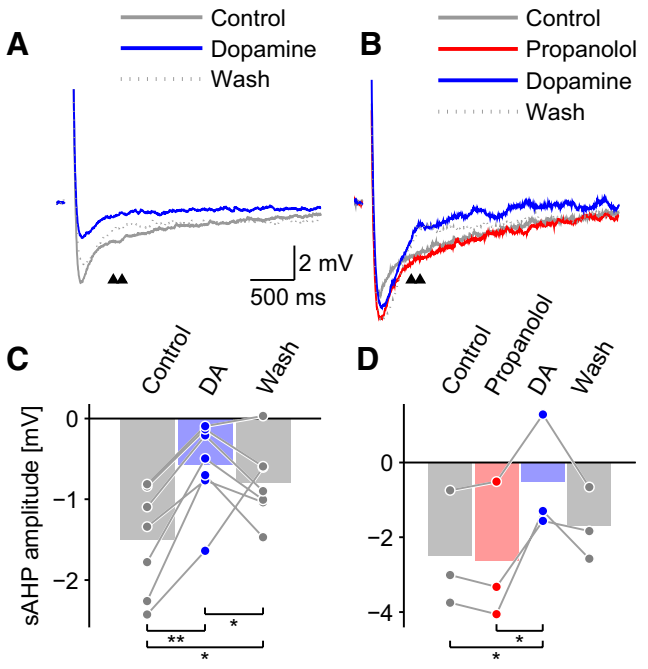

FIG. 4. Dopamine induced decrease of the slow afterhyperpolarization (sAHP). *A*: The sAHP (average of 5 responses) after 30 spikes at 50 Hz in control solution (gray solid line), during DA application at 50 μM (blue solid line), and after washout (gray dashed line). DA reduced the amplitude of the sAHP, which was partially reversible after 30-min wash out. Arrow heads demarcate the part of the voltage trace that was used to estimate the sAHP. We refer to the most hyperpolarized part of the voltage trace as the medium AHP (mAHP). *B*: same protocol as in *A* but under presence of propanolol at 10 μM (red solid line). Propanolol itself augmented the mAHP but did not affect the sAHP. DA still reduced the sAHP but not the mAHP. *C*: the sAHP amplitude for all cells (dots) with related values connected by lines. The data correspond to the example in *A*. The sAHP was quantified between 450 and 550 ms after the last pulse (arrow heads in *A*). Underlying bars are the mean values. Asterisks mark significant differences between indicated pairs: *, $P \leq 0.05$; **, $P \leq 0.01$, paired *t*-test. *D*: same as *C* but under presence of propanolol.

As a second approach, we analyzed the instantaneous firing frequency of PFC pyramidal neurons. LaCamera et al. (2006) showed that slow adaptation in the order of seconds is present in the time course of the instantaneous firing frequency in somatosensory cortex neurons when driven sufficiently strong. Additionally, they observed facilitation in the order of few tens of milliseconds. In contrast, we did not observe facilitation and slow adaption in PFC layer 5 pyramidal neurons (see Fig. 1*B* as an example). The time course of the instantaneous firing frequency comprised solely two decaying components: a very fast initial one in the order of a few milliseconds and a slower component lasting tens of milliseconds. Afterward the response remained stable. We fitted the instantaneous firing rate with two exponential functions to evaluate DA-mediated changes of the time constants of the instantaneous firing rate. DA-mediated influences were, however, not apparent (data not shown).

DA enables and stabilizes persistent activity—mean field analysis

Persistent activity, which is thought to underlie PFC function, is, for example, observed during working-memory tasks (Goldman-Rakic 1995). It is a network phenomenon in that it is assumed to be sustained by reverberating excitatory synaptic activity between recurrently connected cells (see, e.g., Wang 2001). To investigate what the effects of DA on the input-output relationship of PFC pyramidal neurons imply for persistent activity, we subsequently analyze a network of recurrently connected excitatory neurons via a mean field description (Brunel 2000) (see also METHODS).

The excitatory neurons, i.e., pyramidal cells, are described by CLIFF model neurons using average parameters identified from our experimental data for the steady-state response at 100 μM DA. Firing rate adaptation and dopaminergic influences on sAHP are assumed to be at stable values and are not modeled. The cells of the network are assumed to be randomly connected. We also incorporate a spontaneous background activity $f_{sp} = 0.5$ Hz, which is assumed to be unaffected by DA (see METHODS).

Without synaptic input, the activity of our network may be self-sustained inside the neural population by synaptic reverberation, i.e., the network assumes a *stable state*. The stable activity states of the network are identified by the intersection points of the *f-I* curve (*Eq. 2*) with a straight line of slope $1/(cNJ\tau_c)$ and appropriate offset (see Fig. 5*A*, *Eq. 4* and METHODS). Here, c denotes the connectivity, N the number of neurons, and τ_c the decay time constant of single EPSCs. The product cNJ characterizes to the total synaptic current to a cell of the network that comes from recurrent connections. By focusing at the synaptic feedback cNJ rather than just the synaptic coupling strength J, we can discuss the behavior of the network independently of the network size.

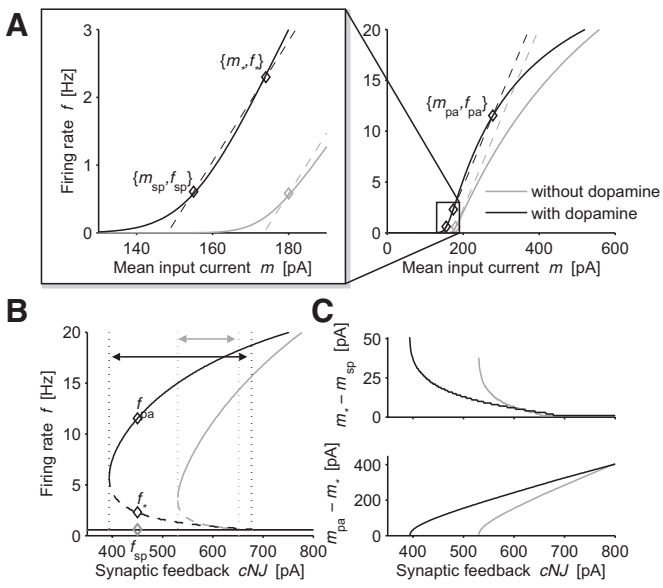

FIG. 5. Mean field description of DA influence on the behavior of a network of excitatory cells. *A*: stable states of the firing rate are intersections between *f-I* curves (solid lines) and a corresponding straight line (dashed, same color, here the synaptic feedback $cNJ = 450$ pA). Diamonds mark stable state values. Cases without DA are shown in gray and with DA in black throughout the figure. *Left*: an extension of the marked area in the *right panel*. *B*: bifurcation diagram showing stable state firing rates as a function of cNJ. Solid lines depict the stable lower and upper fixed points and the dashed line indicates the unstable intermediate fixed point. Diamonds mark stable-state values for a synaptic feedback $cNJ = 450$ pA as in *A*. Dotted lines demarcate the range of values of cNJ with bistability without (gray arrow) and with DA (black arrow). *C, top*: minimum input current above spontaneous input m_{sp} necessary to evoke elevated self-sustained persistent activity as a function of cNJ. *Bottom*: input current necessary to break down persistent activity as a function of cNJ. Parameters are $f_{sp} = 0.5$ Hz, $s = 100$ pA, and $\tau_c = 25$ ms.

Networks of recurrently connected neurons show bistability, i.e., coexistence of spontaneous background activity and elevated persistent activity. Coexistence of a low and a high activity state is a prerequisite to encode information via distinct network states. In networks composed of excitatory units only, bistability is found over a limited range of synaptic feedback *cNJ* (Fusi and Mattia 1999). The emergence of bistability can be understood by means of the graphical approach provided in Fig. 5*A*: for low synaptic feedback *cNJ* the slope of the straight line (*Eq. 4*) is high, only one point of intersection (fixed point) at $\{m_{sp}, f_{sp}\}$ exists, and the network is spontaneously active; as an illustration see the gray *f-I* curve in the case without DA in Fig. 5*A*. Increasing the synaptic feedback *cNJ*—either by increasing the effective number of connections *cN* or the synaptic strength *J*—decreases the slope of the line, and above a certain value of *cNJ*, one finds three points of intersection; as an illustration see the black *f-I* curve in Fig. 5*A,* which shows the case with DA. The lower point still corresponds to stable spontaneous activity, the intermediate one $\{m_*, f_*\}$ belongs to an unstable state and the upper intersection to stable persistent activity $\{m_{pa}, f_{pa}\}$. Due to the two stable fixed points, we have bistability between spontaneous and persistent activity at these values of *cNJ*, i.e., the network can reside self-sustained in one of the two states. Further increase of synaptic feedback *cNJ* results in the lower and middle fixed points merging together and becoming unstable. Only the upper intersection remains stable and reflects nontriggered high-frequency persistent network activity.

How does the dopaminergic modulation of the *f-I* curve, i.e., the rheobase reduction, the gain increase and the stronger saturation, influence the state space description? Due to our assumption that the spontaneous firing rate f_{sp} remains the same for dopaminergic and nondopaminergic cases, a shift of the *f-I* curve to lower current values by DA does not change the stable states, i.e., the points of intersection. Thus a simple excitability increase through rheobase reduction does not affect persistent activity at all. However, a DA-induced gain increase allows for persistent activity at lower synaptic strengths (Fig. 5*B*). Because a gain increase acts as a factor in front of the synaptic feedback *cNJ*, the result is a left shift of the *f-cNJ* curve to lower values of synaptic feedback *cNJ*. Persistent activity becomes more stable because the basin of attraction of the upper fixed point widens.

To quantify the above-mentioned effects, we extracted the minimal current needed to push the network from low spontaneous activity to high persistent activity. Figure 5*C, top,* shows for each value of the synaptic feedback *cNJ* the current $m_* - m_{sp}$ above spontaneous levels required to reach the basin of attraction for the persistent activity state. This is reached as soon as the total synaptic current crosses the value m_* corresponding to the unstable fixed point. As reflected by the graph, DA enables persistent activity at much lower values of *cNJ*, and less input current is required to reach this state. DA also widens the basin of attraction for the persistent activity state, represented by the current difference between persistent and unstable fixed point, $m_{pa} - m_*$ (Fig. 5*C, bottom*). This current difference is also the minimal negative, i.e., inhibitory, current required to move the network out of the attraction domain for persistent activity. In the presence of DA, stronger distractor currents are needed to irrecoverably perturb persistent activity. Note that aside from the external contribution, the currents m_{sp}, m_*, m_{pa} and their differences (Fig. 5*C*) contain a contribution from the recurrent network and do not directly correspond to the external currents necessary to evoke or interrupt persistent activity.

Interestingly, DA acts in a nonlinear way on the *f-I* curve which goes beyond pure gain modulation. If DA would only act as a constant gain factor, the range of *cNJ* that allows for bistability would only marginally increase; because a pure gain increase moves also, the point where spontaneous activity state and unstable fixed point merge to lower values of *cNJ*. However, in our experiments, DA increased the input resistance of PFC pyramidal neurons. Larger input resistance results in larger fluctuations of the membrane potential for the same fluctuations of the input current. Therefore the initial part of the *f-I* curve at low-frequency values, i.e., close to f_{sp}, extends over a larger range of mean input currents *m* (Fig. 5A). At the network level the point where spontaneous activity state and unstable fixed point merge becomes shifted to larger values of *cNJ*. Thus the range of synaptic feedback *cNJ* with bistability widens (dotted lines and arrows in Fig. 5*B*), i.e., bistability becomes more robust against fluctuations in the network parameters.

We conclude that DA application increases the range of synaptic strengths *J* that allow for network bistability. At the same time, DA makes the high activity state more stable against distractors.

DA enables and stabilizes persistent activity—simulations

As an example of the implications of dopaminergic modulation of the input-output relationship of PFC pyramidal neurons, we provide simulations of a recurrently connected network of excitatory integrate-and-fire neurons. The pyramidal cells are described by CLIFF neurons using parameters identified from the 13 cells in our experimental data for a DA concentration of 100 μM. The number of neurons was increased 20 times to $n = 260$ with a connection probability $c = 0.1$ (see METHODS). To be more biologically plausible, we incorporate a spontaneous activity of 0.5 Hz.

First, synaptic weights *J* are set in such a way that the neurons of the network start firing due to an external trigger, i.e., stimulus current in form of a square pulse underlying noisy background current delivered to each neuron. After stimulus removal, activity ceases without DA (Fig. 6*A*) but not in presence of DA (Fig. 6*B*). Hence DA enabled, but did not evoke, persistent activity in the example. Note that firing stabilizes at lower rate after stimulus removal than during stimulus presentation (Fig. 6*B*). The lower firing rate corresponds to a stable state between input and output within the network in absence of external input (Amit and Brunel 1997).

Second, we increase synaptic weights *J* so that persistent activity is provoked without and with DA (Fig. 6, *C* and *D*). However, distracting input disrupts persistent activity without DA (Fig. 6*C*), whereas with DA (Fig. 6*D*), persistent activity remains and the working-memory item is not erased. DA therefore stabilizes persistent activity in the example. Distracting input is modeled as a negative current injection into every neuron. Note that the only way to silence, i.e., *distract* in our case, the activity of an attractor neuronal network that resides in its "high activity" fixed point, is via negative current injection (cf. *DA enables and stabilizes persistent activity—mean*

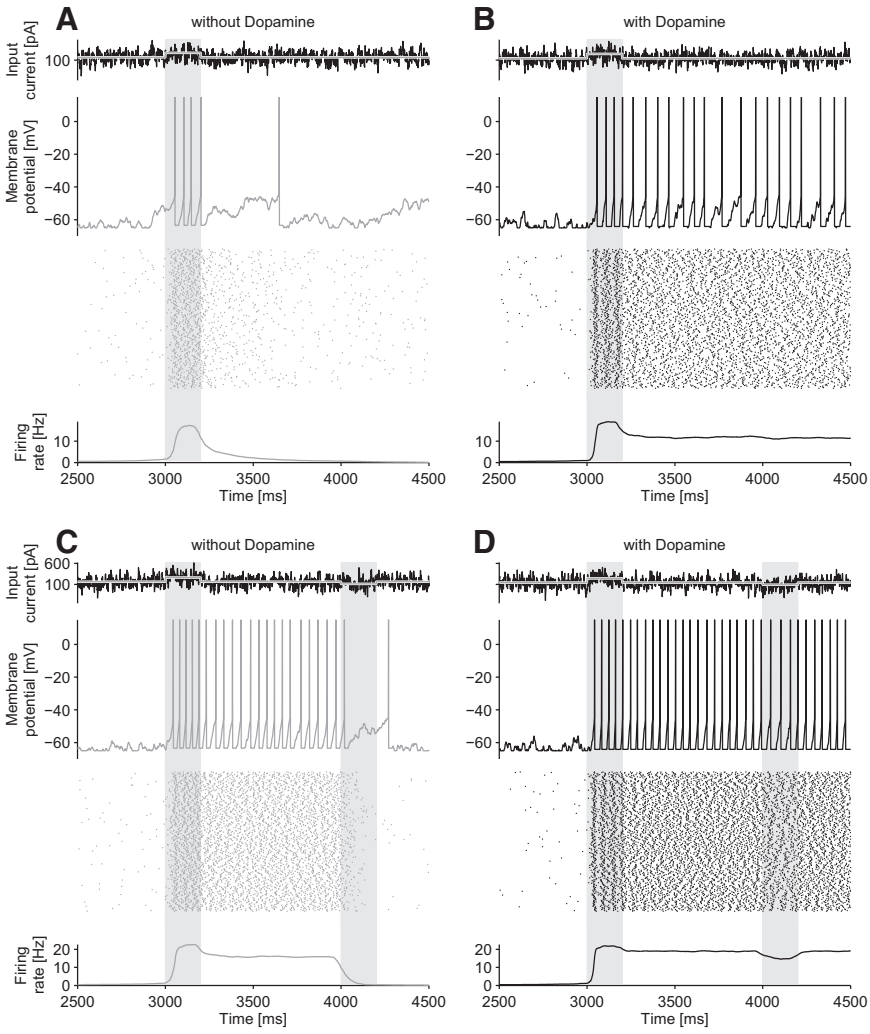

FIG. 6. Dopamine enables and stabilizes persistent activity. *A–D, top*: the injected current, i.e., noisy background and the mean input current (overlayed in gray) with square pulses for working memory item and distractor, respectively. *Second panel*: voltage trace of one example neuron; *third panel*: output spikes (dots) of the whole network (1 row corresponds to 1 of the 260 cells); *bottom*: the mean firing rate of the whole network. *A* and *B*: with synaptic weights $J = 17$ pA, injection of a 100-pA current pulse for 200 ms (gray shaded area) does not provoke persistent activity without (*A*) but in presence of dopamine (*B*). *C* and *D*: with synaptic weights $J = 25$ pA, persistent activity is found in both cases but breaks down by injection of distracting input (−50 pA, 200 ms) without dopamine. Parameters are $f_{sp} = 0.5$ Hz, $s = 100$ pA.

field analysis and Fig. 5*C*). In the present model, negative current might represent input from inhibitory neurons. These inhibitory cells may themselves be activated by a competing population of pyramidal neurons that respond to another stimulus (to keep things simple not explicitly modeled here).

DISCUSSION

We investigated the DA-mediated modulation of the input-output function of layer 5 pyramidal neurons in rat prefrontal cortex. Bath application of DA increased the excitability of pyramidal cells by reducing the rheobase current and increasing the gain of the input-output function. The DA-induced effects were found to be largely mediated by D1 receptor activation. We, however, cannot completely rule out a contribution of nondopaminergic receptors, e.g., β-adrenergic receptors, activated by the high DA concentrations (25–100 μM). For strong and long stimulation exceeding 2 s, the maximum firing rate was decreased. Incorporating these findings into a recurrently connected network of model pyramidal neurons, we could show that the experimentally observed dopaminergic modulation of the input-output function facilitates and stabilizes persistent activity. Our results confirm the original hypothesis of Servan-Schreiber et al. (1990) that catecholamines modulate the gain of the neuronal input-output function.

DA-mediated increase of excitability

Dopaminergic enhancement of pyramidal cell excitability via D1 receptor stimulation in the PFC has previously been reported. A considerable amount of in vitro studies revealed increased excitability after bath application of DA, a D1 receptor agonist (Henze et al. 2000; Lavin and Grace 2001; Shi et al. 1997; Tseng and O'Donnell 2004; Wang and O'Donnell 2001; Yang and Seamans 1996) or synaptically evoked DA release from VTA projections (Chen et al. 2007; Lavin et al. 2005; Lewis and O'Donnell 2000). Most studies, including our own, made use of (pre-)pubertal animals. However, DA modulation of PFC function has been shown to be age-dependent in that some DA effects change after puberty (Tseng and O'Donnell 2005). We can therefore not rule out that our results may change for adult animals.

DA modulation of PFC neurons has further been reported to comprise "transient" (on a scale of seconds) and longer-lasting components (Geijo-Barrientos and Pastore 1995; Gulledge and Jaffe 1998; Rotaru et al. 2007; Seamans and Yang 2004; Seamans et al. 2001b), suggesting that excitability may initially decrease but then reverse and stabilize at a higher level. We performed similar experiments, using a fixed amount of input current as in previous studies, to investigate the time course of the excitability modulation by

DA. Application of DA under blockade of synaptic inputs led to an excitability increase in our experiments but without a preceding transient reduction. Similar findings were made by others (Gulledge and Jaffe 2001). The excitability increase was stable after 5 min of DA application up to 25 minutes. Afterward, a slow excitability decrease appeared, suggesting receptor desensitization.

Indications for a DA-induced gain modulation in PFC layer 5 pyramidal neurons were already reported by Lavin and Grace (2001). Using square pulses of few hundred milliseconds, they compared responses of cells intermediately clamped at de- or hyperpolarized membrane potentials that were supposed to mimic cortical up and down states. They found a gain increase after DA administration for both membrane potential states. However, Lavin and Grace (2001) showed their gain increase only for a range of input of several tens of picoampere. We could confirm these findings and extend them over a broad range of input currents of several hundred picoampere.

The barrage of synaptic input a neuron experiences in vivo is characterized by large random fluctuations rather than a DC input. But noisy inputs have been shown to reduce the gain of the neuronal response function (Chance et al. 2002; Rauch et al. 2003; Shu et al. 2003), potentially counteracting DA-mediated gain increase. Using fluctuating input currents, we could show that, nevertheless a DA-induced gain increase is preserved for different amounts of input fluctuations.

Working-memory activity is believed to be formed by self-sustained network activity in prefrontal cortex. Insight into the ability of a neuronal network to sustain activity over prolonged periods of time requires responses to long-lasting neuronal stimuli. With long-lasting stimulation extending across seconds, we showed that the gain of the neural response function depends on the duration of the stimulation, a finding recently reported also in somatosensory cortex neurons (Higgs et al. 2006). The amount of gain change induced by DA, however, was not different between early (transient) and subsequent response phases.

DA effects on the input-output response function were associated with a depolarization of the membrane potential of PFC pyramidal neurons in agreement with previous reports (Gulledge and Jaffe 1998; Shi et al. 1997; but see Henze et al. 2000; Yang and Seamans 1996). However, in our experiments, membrane potential depolarization was not required for gain increase by DA. Holding the membrane potential constant before and during DA application did not occlude DA-mediated gain increase in control experiments.

Dopaminergic modulation of PFC pyramidal cell excitability has largely been reported to be due to changes of synaptic input (Gulledge and Jaffe 2001; Tseng and O'Donnell 2004; Wang and O'Donnell 2001) or intrinsic currents, e.g., persistent sodium current, persistent potassium current and calcium currents (Yang et al. 1996; Gorelova and Yang 2000; Chen et al. 2007). By systematically blocking all synaptic inputs, we intended to focus solely on single cell properties amenable to DA modulation. Our results suggest the involvement of currents that contribute to slow sAHP and slow spike frequency adaptation.

Involvement of D1, D2, and nondopaminergic receptors

D1 receptors are the predominant receptors at prefrontal pyramidal neurons (Goldman-Rakic et al. 2000) and excitability increases were shown in vitro to be mediated by D1 receptor activation (e.g., Chen et al. 2007; Tseng and O'Donnell 2004; Wang and O'Donnell 2001;). Excitability decreases are mostly due to increased inhibition mediated by D2 receptor activation located on interneurons (e.g., Gulledge and Jaffe 2001). In the present study, the specific D1 receptor agonist, SKF 38393, modulated the input-output relationship of pyramidal neurons similar to the action of DA itself, but the agonist did not increase the membrane resting potential. A reduction of the rheobase current was also present under application of the specific D2 receptor agonist, quinpirole, but was not accompanied by the other features found with DA application and in particular a gain increase was not present. The D1 receptor antagonist SCH 23390 occluded the influences of DA on the *f-I* curve. Blocking β-adrenergic receptors with propanolol, however, reduced the effects of DA somewhat but not completely. These findings indicate that the modulation of the *f-I* curve by DA is mainly mediated by D1 receptors.

Both D1 and D2 agonists increased the input resistance, accounting for the rheobase reduction under DA application. The additional depolarization observed under DA application might not be due to D1 or D2 receptor activation but another mechanism (Shi et al. 1997). This was confirmed by co-application of DA and a D2 receptor antagonist: the cell depolarized, in addition to a rheobase-reduction, a gain increase, and a decrease of the maximum frequency.

We conclude that it is mainly the D1 receptor that mediates the tonic effects of DA on the input-output relationship of layer 5 pyramidal neurons in the PFC. A cross-activation of nondopaminergic receptors can, however, not be entirely excluded.

DA effects onto slow spike frequency adaptation and the relationship to gain increase

The AHP following repetitive firing is composed of a fast (fAHP, up to few milliseconds), medium (mAHP, up to several hundred milliseconds), and slow component (sAHP, up to several seconds) with the peak of the hyperpolarization a few milliseconds after the peak of the action potential (Sah and Faber 2002). The slow AHP component reflects Ca^{2+}- and Na^{+}-dependent K^{+} conductances that are involved in spike frequency adaptation (see e.g., Higgs et al. 2006; Sah and Faber 2002; Viana et al. 1993) and therefore possibly take part in the modulation of neuronal output rates. DA has been reported to modulate the AHP in the striatum (Nicola et al. 2000) and induce a slow afterdepolarization in the amygdala (Yamamoto et al. 2007). At the time, however, there is no evidence that DA modulates Ca^{2+}- and Na^{+}-dependent K^{+} conductances in the PFC (Seamans and Yang 2004). In contrast to our results, the absence of DA effects on the (slow) AHP has been reported (Lavin and Grace 2001). A sAHP, however, is reliably found only after repetitive firing at high firing rate (Higgs et al. 2006; Zhang and Arsenault 2005). Using a protocol with strong drive of the PFC layer 5 pyramidal neurons (Higgs et al. 2006), we could show that DA nevertheless reduces the sAHP. Reduction of the sAHP was shown to be related to gain increase in prefrontal pyramidal

neurons (Zhang and Arsenault 2005), in somatosensory pyramidal neurons (Higgs et al. 2006), and also in hypoglossal motoneurons (Viana et al. 1993). We therefore presume that a reduction of the sAHP amplitude might underlie gain increase in layer 5 pyramidal neurons of the PFC.

Dopaminergic reduction of the AHP has been suggested to arise from a cross-activation of β-adrenergic receptors in hippocampal pyramidal neurons (Malenka and Nicoll 1986). No cross-activation was, however, reported by Pedarzani and Storm (1995). We tested whether cross-activation might underlie AHP reduction by DA in our experiments with PFC pyramidal neurons. Blocking β-adrenergic receptors with propanolol, in fact largely abolished DA effects on the medium part of the AHP. However, the sAHP was still substantially reduced by DA. The sAHP reduction by DA could, however, not be completely blocked by co-application of the D1 receptor antagonist SCH 23390. Thus the relevance of the sAHP for gain increase and the importance of D1 and/or other receptors in the relationship between both features is not entirely clear and needs further clarification.

DA-mediated facilitation and stabilization of persistent activity

The fit of the *f-I* curve with an integrate-and-fire model neuron allowed us to study the DA effects in a recurrently connected network model. Previous modeling studies provide detailed insight into the concept of stabilizing delay-type activity by DA in the PFC (e.g., Braver et al. 1999; Brunel and Wang 2001; Compte et al. 2000; Dreher and Burnod 2002; Durstewitz et al. 2000a). These studies, however, mainly focused on the dopaminergic modulation of synaptic inputs found in previous experimental studies (e.g., Gao and Goldman-Rakic 2003; Gao et al. 2001, 2003; Seamans et al. 2001a,b). Our findings support and extend the insights offered by these studies: DA stabilizes persistent network activity against distracting input by a gain increase of the neuronal input-output function. This is achieved by enlarging the basins of attraction of the persistent activity state.

We conclude that the effects of DA on the neuronal input-output function reported here functionally match the previously described effects of DA on synaptic transmission in the PFC. In view of the diversity of results on DA modulation of PFC function (e.g., Seamans and Yang 2004), this reveals a remarkable convergence between the DA modulation of single neurons and synapses on the level of the network.

ACKNOWLEDGMENTS

We thank T. Berger, M. Giugliano, D. Ledergerber, and R. Urbanczik for valuable discussion and comments on the manuscript.

GRANTS

This work was supported by Swiss National Science Foundation Grant 31-61335.00 to H.-R. Lüscher.

REFERENCES

Aggelopoulos NC, Franco L, Rolls ET. Object perception in natural scenes: encoding by inferior temporal cortex simultaneously recorded neurons. *J Neurophysiol* 93: 1342–1357, 2005.

Amit DJ, Brunel N. Model of global spontaneous activity and local structured activity during delay periods in the cerebral cortex. *Cereb Cortex* 7: 237–252, 1997.

Arsiero M, Lüscher HR, Lundstrom BN, Giugliano M. The impact of input fluctuations on the frequency-current relationships of layer 5 pyramidal neurons in the rat medial prefrontal cortex. *J Neurosci* 27: 3274–3284, 2007.

Braver TS, Barch DM, Cohen JD. Cognition and control in schizophrenia: a computational model of dopamine and prefrontal function. *Biol Psychiatry* 46: 312–328, 1999.

Brunel N. Persistent activity and the single-cell frequency-current curve in a cortical network model. *Network* 11: 261–280, 2000.

Brunel N, Wang XJ. Effects of neuromodulation in a cortical network model of object working memory dominated by recurrent inhibition. *J Comput Neurosci* 11: 63–85, 2001.

Chance FS, Abbott LF, Reyes AD. Gain modulation from background synaptic input. *Neuron* 35: 773–782, 2002.

Chen L, Bohanick JD, Nishihara M, Seamans JK, Yang CR. Dopamine D1/5 receptor-mediated long-term potentiation of intrinsic excitability in rat prefrontal cortical neurons: Ca^{2+}-dependent intracellular signaling. *J Neurophysiol* 97: 2448–2464, 2007.

Cohen JD, Braver TS, Brown JW. Computational perspectives on dopamine function in prefrontal cortex. *Curr Opin Neurobiol* 12: 223–229, 2002.

Compte A, Brunel N, Goldman-Rakic PS, Wang XJ. Synaptic mechanisms and network dynamics underlying spatial working memory in a cortical network model. *Cereb Cortex* 10: 910–923, 2000.

Compte A, Constantinidis C, Tegner J, Raghavachari S, Chafee MV, Goldman-Rakic PS, Wang XJ. Temporally irregular mnemonic persistent activity in prefrontal neurons of monkeys during a delayed response task. *J Neurophysiol* 90: 3441–3454, 2003.

Destexhe A, Paré D. Impact of network activity on the integrative properties of neocortical pyramidal neurons in vivo. *J Neurophysiol* 81: 1531–1547, 1999.

Dreher JC, Burnod Y. An integrative theory of the phasic and tonic modes of dopamine modulation in the prefrontal cortex. *Neural Netw* 15: 583–602, 2002.

Durstewitz D, Seamans JK. The computational role of dopamine D1 receptors in working memory. *Neural Netw* 15: 561–572, 2002.

Durstewitz D, Seamans JK, Sejnowski TJ. Dopamine-mediated stabilization of delay-period activity in a network model of prefrontal cortex. *J Neurophysiol* 83: 1733–1750, 2000a.

Durstewitz D, Seamans JK, Sejnowski TJ. Neurocomputational models of working memory. *Nat Neurosci* 3, *Suppl*: 1184–1191, 2000b.

Fleidervish IA, Friedman A, Gutnick MJ. Slow inactivation of Na^+ current and slow cumulative spike adaptation in mouse and guinea-pig neocortical neurones in slices. *J Physiol* 493: 83–97, 1996.

Fusi S, Mattia M. Collective behavior of networks with linear (VLSI) integrate-and-fire neurons. *Neural Comput* 11: 633–652, 1999.

Gao WJ, Goldman-Rakic PS. Selective modulation of excitatory and inhibitory microcircuits by dopamine. *Proc Natl Acad Sci USA* 100: 2836–2841, 2003.

Gao WJ, Krimer LS, Goldman-Rakic PS. Presynaptic regulation of recurrent excitation by D1 receptors in prefrontal circuits. *Proc Natl Acad Sci USA* 98: 295–300, 2001.

Gao WJ, Wang Y, Goldman-Rakic PS. Dopamine modulation of perisomatic and peridendritic inhibition in prefrontal cortex. *J Neurosci* 23: 1622–1630, 2003.

Geijo-Barrientos E, Pastore C. The effects of dopamine on the subthreshold electrophysiological responses of rat prefrontal cortex neurons in vitro. *Eur J Neurosci* 7: 358–366, 1995.

Goldman-Rakic PS. Cellular basis of working memory. *Neuron* 14: 477–485, 1995.

Goldman-Rakic PS, Muly EC, Williams GV. D1 receptors in prefrontal cells and circuits. *Brain Res Brain Res Rev* 31: 295–301, 2000.

Gorelova NA, Yang CR. Dopamine D1/D5 receptor activation modulates a persistent sodium current in rat prefrontal cortical neurons in vitro. *J Neurophysiol* 84: 75–87, 2000.

Gulledge AT, Jaffe DB. Dopamine decreases the excitability of layer V pyramidal cells in the rat prefrontal cortex. *J Neurosci* 18: 9139–9151, 1998.

Gulledge AT, Jaffe DB. Multiple effects of dopamine on layer V pyramidal cell excitability in rat prefrontal cortex. *J Neurophysiol* 86: 586–595, 2001.

Henze DA, González-Burgos GR, Urban NN, Lewis DA, Barrionuevo G. Dopamine increases excitability of pyramidal neurons in primate prefrontal cortex. *J Neurophysiol* 84: 2799–2809, 2000.

Higgs MH, Slee SJ, Spain WJ. Diversity of gain modulation by noise in neocortical neurons: regulation by the slow afterhyperpolarization conductance. *J Neurosci* 26: 8787–8799, 2006.

LaCamera G, Rauch A, Thurbon D, Lüscher HR, Senn W, Fusi S. Multiple time scales of temporal response in pyramidal and fast spiking cortical neurons. *J Neurophysiol* 96: 3448–3464, 2006.

LaCamera G, Senn W, Fusi S. Comparison between networks of conductance- and current-driven neurons: stationary spike rates and subthreshold depolarization. *Neurocomputing* 58–60: 253–258, 2004.

Larkum ME, Senn W, Lüscher HR. Top-down dendritic input increases the gain of layer 5 pyramidal neurons. *Cereb Cortex* 14: 1059–1070, 2004.

Lavin A, Grace AA. Stimulation of D1-type dopamine receptors enhances excitability in prefrontal cortical pyramidal neurons in a state-dependent manner. *Neuroscience* 104: 335–346, 2001.

Lavin A, Nogueira L, Lapish CC, Wightman RM, Phillips PEM, Seamans JK. Mesocortical dopamine neurons operate in distinct temporal domains using multimodal signaling. *J Neurosci* 25: 5013–5023, 2005.

Lewis BL, O'Donnell P. Ventral tegmental area afferents to the prefrontal cortex maintain membrane potential "up" states in pyramidal neurons via D1 dopamine receptors. *Cereb Cortex* 10: 1168–1175, 2000.

Malenka RC, Nicoll RA. Dopamine decreases the calcium-activated afterhyperpolarization in hippocampal CA1 pyramidal cells. *Brain Res* 379: 210–215, 1986.

Nicola SM, Surmeier J, Malenka RC. Dopaminergic modulation of neuronal excitability in the striatum and nucleus accumbens. *Annu Rev Neurosci* 23: 185–215, 2000.

Pedarzani P, Storm JF. Dopamine modulates the slow Ca(2+)-activated K^+ current I_{AHP} via cyclic AMP-dependent protein kinase in hippocampal neurons. *J Neurophysiol* 74: 2749–2753, 1995.

Rauch A, LaCamera G, Lüscher HR, Senn W, Fusi S. Neocortical pyramidal cells respond as integrate-and-fire neurons to in-vivo-like input currents. *J Neurophysiol* 90: 1598–1612, 2003.

Rotaru DC, Lewis DA, Gonzalez-Burgos G. Dopamine D1 receptor activation regulates sodium channel-dependent EPSP amplification in rat prefrontal cortex pyramidal neurons. *J Physiol* 581: 981–1000, 2007.

Sah P, Faber ESL. Channels underlying neuronal calcium-activated potassium currents. *Prog Neurobiol* 66: 345–353, 2002.

Salinas E, Sejnowski TJ. Gain modulation in the central nervous system: where behavior, neurophysiology, and computation meet. *Neuroscientist* 7: 430–440, 2001.

Sawaguchi T, Goldman-Rakic PS. D1 dopamine receptors in prefrontal cortex: involvement in working memory. *Science* 251: 947–950, 1991.

Seamans JK, Durstewitz D, Christie BR, Stevens CF, Sejnowski TJ. Dopamine D1/D5 receptor modulation of excitatory synaptic inputs to layer V prefrontal cortex neurons. *Proc Natl Acad Sci USA* 98: 301–306, 2001a.

Seamans JK, Gorelova NA, Durstewitz D, Yang CR. Bidirectional dopamine modulation of GABAergic inhibition in prefrontal cortical pyramidal neurons. *J Neurosci* 21: 3628–3638, 2001b.

Seamans JK, Yang CR. The principal features and mechanisms of dopamine modulation in the prefrontal cortex. *Prog Neurobiol* 74: 1–58, 2004.

Servan-Schreiber D, Printz H, Cohen JD. A network model of catecholamine effects: gain, signal-to-noise ratio, and behavior. *Science* 249: 892–895, 1990.

Shi WX, Zheng P, Liang XF, Bunney BS. Characterization of dopamine-induced depolarization of prefrontal cortical neurons. *Synapse* 26: 415–422, 1997.

Shu Y, Hasenstaub A, Badoual M, Bal T, McCormick DA. Barrages of synaptic activity control the gain and sensitivity of cortical neurons. *J Neurosci* 23: 10388–10401, 2003.

Tang AC, Bartels AM, Sejnowski TJ. Effects of cholinergic modulation on responses of neocortical neurons to fluctuating input. *Cereb Cortex* 7: 502–509, 1997.

Tseng KY, O'Donnell P. Dopamine-glutamate interactions controlling prefrontal cortical pyramidal cell excitability involve multiple signaling mechanisms. *J Neurosci* 24: 5131–5139, 2004.

Tseng KY, O'Donnell P. Post-pubertal emergence of prefrontal cortical up states induced by D1-NMDA co-activation. *Cereb Cortex* 15: 49–57, 2005.

Viana F, Bayliss DA, Berger AJ. Multiple potassium conductances and their role in action potential repolarization and repetitive firing behavior of neonatal rat hypoglossal motoneurons. *J Neurophysiol* 69: 2150–2163, 1993.

Wang J, O'Donnell P. D1 dopamine receptors potentiate NMDA-mediated excitability increase in layer V prefrontal cortical pyramidal neurons. *Cereb Cortex* 11: 452–462, 2001.

Wang XJ. Synaptic basis of cortical persistent activity: the importance of NMDA receptors to working memory. *J Neurosci* 19: 9587–9603, 1999.

Wang XJ. Synaptic reverberation underlying mnemonic persistent activity. *Trends Neurosci* 24: 455–463, 2001.

Yamamoto R, Ueta Y, Kato N. Dopamine induces a slow afterdepolarization in lateral amygdala neurons. *J Neurophysiol* 98: 984–992, 2007.

Yang CR, Seamans JK. Dopamine D1 receptor actions in layers V-VI rat prefrontal cortex neurons in vitro: modulation of dendritic-somatic signal integration. *J Neurosci* 16: 1922–1935, 1996.

Yang CR, Seamans JK, Gorelova NA. Electrophysiological and morphological properties of layers V-VI principal pyramidal cells in rat prefrontal cortex in vitro. *J Neurosci* 16: 1904–1921, 1996.

Zhang Z. Maturation of layer V pyramidal neurons in the rat prefrontal cortex: intrinsic properties and synaptic function. *J Neurophysiol* 91: 1171–1182, 2004.

Zhang Z, Arsenault D. Gain modulation by serotonin in pyramidal neurons of the rat prefrontal cortex. *J Physiol* 566: 379–394, 2005.